The influence of processing conditions on the aesthetical, morphological and mechanical properties of SF mouldings of high-impact polystyrene (HIPS-SF)

F. R. Esteves, T.A. Carvalho, A. S. Pouzada & C. I. Martins
Institute for Polymer and Composites/I3N, University of Minho, Guimarães, Portugal

ABSTRACT: The production of large plastic parts, in small series and at low cost, requires the development of alternative tools and materials. Structural foams (SF) are a good solution, when the production of thicker parts with good properties is the specification. They allow obtaining lightweight parts with high stiffness and good dimensional stability, due to their sandwich-like structure constituted by a cellular core and two solid skins. The porous core results from the addition of a blowing agent in the polymeric matrix. These materials are applied in urban furniture, automotive, nautical and aerospace industries. The most used process to produce SF is the low pressure foam moulding, which is a short shot process, with impression pressures ranging from 1.4 to 4 MPa. Thus, the use of hybrid moulds with moulding blocks obtained by rapid prototyping routes is seen as a viable alternative for SF injection moulding.
This work reports on a study of the influence of processing conditions on the aesthetical, morphological, and mechanical properties of SF mouldings of high-impact polystyrene (HIPS-SF). The results compare the effect of the use of hybrid moulds to conventional moulds on the surface aspect of the circular centre gated mouldings. Furthermore the influence of the moulding temperature is ascertained in terms of the resulting cellular morphology, the flexural stiffness of the plate mouldings, and the impact resistance in the instrumented drop weight test.

1 INTRODUCTION

Structural foams (SF) are multi-layer materials consisting of two integral skins and a cellular core (Malloy 1994; Rosato et al. 2000). This structure combines the lightness of the cellular core with the strength of the unfoamed skins. The most important characteristic of this sandwich structure is its high specific flexural stiffness/strength ratio. For this reason, the main use of this structure is in engineering and load-bearing applications (Barzegari and Rodrigue 2009a).

Thermoplastic SF may be produced by a variety of injection moulding techniques. Commonly, SF are manufactured by a low pressure short-shot process (typically 65 to 90% of the impression volume), in which an amount of melt containing dissolved gas (usually chemical blowing agents (CBA)) is injected to partially fill the impression (Ahmadi and Hornsby 1984). This process has advantages like: the possibility of production of complex thick and large parts without sink marks; the development of low level of internal stresses; less tendency to warpage and distortion; and requirement of reduced clamping forces due to the low impression pressures, typically below 4 MPa (Nogueira et al. 2011; Rosato et al. 2000). Conversely the cycle time is longer, the surface finish is poor, there is emission of gases during processing, and reprocessing is more complex (Barzegari and Rodrigue 2009a).

The complex inter-relationship between structure properties and moulding conditions have already been discussed in depth by Ahmadi *et al.* (Ahmadi and Hornsby 1984). They concluded that the uniformity and fineness of the cellular core is greater when using high injection rates combined with low melt and mould temperatures. The poor uniformity in cell distribution in mouldings injected by the low pressure process is largely attributed to the deficient mixing of the CBA and the polymer. In certain regions of the moulding there is coalescence of numerous small cells. It is difficult to control the cell size and cell size distribution (Kamal et al. 2009; Mark 2007). The size and density of the cells, the skin thickness and the density profile across the thickness have a considerable effect on the mechanical properties of the resulting foams. CBA concentration and injection pressure are the main factors influencing foam quality. The mould temperature has a significant effect on skin thickness; back pressure also influences skin thickness, cell size and foam

density. Finally, the mould and melt temperatures have negligible effect on the cell density (Barzegari and Rodrigue 2009a).

The flexural stiffness and the impact strength of PP-SF increase with the moulding thickness, the flexural properties depending on whether the SF layered structure is symmetric or asymmetric (Barzegari and Rodrigue 2009b; Tovar-Cisneros et al. 2008). The energy required for crack initiation and the total energy for failure are greatly reduced by the occurrence of microcells in the outer skins that act as stress raisers (Ahmadi and Hornsby 1984; Ahmadi and Hornsby 1985).

The injection moulding of SF is a low pressure process, ideal for the production of large area parts. Therefore, it is a viable candidate for light moulding tools, as it is the case of hybrid moulds (Pouzada 2009). In these tools, the moulding blocks are produced by rapid prototyping and tooling (RPT) such as the vacuum casting of epoxy composites. Typically these blocks are produced on epoxy resin with aluminium powder, that have the advantages of easy manufacturing and short delivery time (Bareta et al. 2007). The main disadvantages, when compared with conventional steel moulds, are the worst thermal and mechanical behaviours, shorter useful lifetime of moulding blocks and longer cycle time, that recommend this processing option for limited number of parts (Pouzada 2009).

This study focus on the morphological and mechanical properties of injected HIPS-SF mouldings. Flexural and impact behaviour of SF are related with morphological and physical parameters, as skin ratio and density. Finally, the experimental results of flexural stiffness are compared to the models proposed by Barzegari *et al* 2007.

2 EXPERIMENTAL

2.1 *Raw materials*

High impact polystyrene (HIPS) from BASF, Korea, with specific gravity of 1.05 $Mg.m^{-3}$ and MFI of 10.95 g/10min (200ºC / 5 kg) was used. 2wt% of an endothermic CBA, Tracel IMC 4200SP, from Tramaco, Germany, with a decomposition temperature in the range of 160-220ºC, was incorporated to the polymeric matrix.

2.2 *Injection moulding*

Centred gated discs of 155 mm in diameter and 5 mm in thickness were processed with an injection moulding machine Engel Victory Spex 50 (Engel, Austria). The mouldings were produced using two mould material combinations: a conventional steel mould configuration and a hybrid mould. The hybrid mould has an insulating plate (resin filled with glass fibres) in the injection side and a moulding block in the ejection side made in a composite of epoxy Biresin L74 filled with 60wt% aluminium powder as described in Figure 1. This moulding block was produced by vacuum casting and machined to the final geometry of the part, following the standard routine described in (Vasconcelos et al. 2004).

The mouldings were injected with 90% of mould filling and the complete filling was promoted by the CBA expansion. Various processing conditions were used, as it is shown in Table 1.

Table 1. Injection moulding processing conditions

Parameter			**Hybrid**	**Steel**
Injection temperature [ºC]		T_{inj}	200 220 240	220
Mould temperature [ºC]	Core	T1	45	75
	Cavity	T2	50	75
Cooling time [s]		t_{cool}	180	80
Flow rate [cm^3/s]		Q	60	

2.3 *Mould monitoring*

The two halves of the mould were instrumented with Resitec type J, TC.002 thermocouples (Resitec, Portugal): one was placed in the injection side at 2 mm of the moulding surface and at 30 mm from the gate (T1), and another in the ejection side, at the same position (T2) (Fig. 1). The signals were acquired and recorded with a data acquisition system Priamus Multi DAQ 8101A.

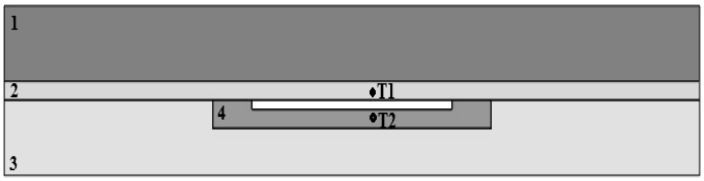

Figure1. Hybrid mould configuration and setup of thermocouples: 1-steel injection plate; 2-insulating plate; 3-steel ejection plate; 4-moulding block (resin or steel).

These thermocouples were placed in these positions to allow the monitoring of the mould temperature, to ensure a symmetric development of the moulding structure (Tovar-Cisneros et al. 2008).

2.4 *Morphological analysis*

An optical microscope Olympus BH-2 (Olympus, Japan) coupled with a digital camera Leica DFC 280 (Leica, Germany) was used to access to the effect of the processing conditions on the microstructural development of the HIPS-SF parts. Thin slices of about 10 µm were microtomed in samples at 30 mm from the gate as shown in Fig. 2. The slices were placed between a glass slide and cover glass after immersion in Canada balsam.

Measurements of the skin ratio were made throughout the section. The skin ratio was defined as

the ratio between the sum of the thickness of the two skin layers and the overall thickness of the samples, expressed as a percentage.

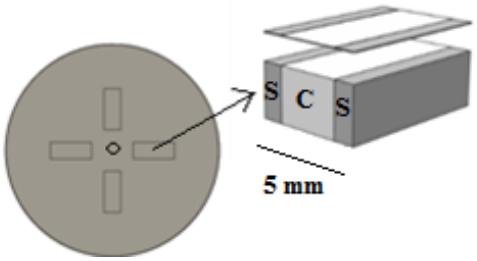

Figure 2. Sample location for the morphological analysis. Insert refers to the slices made along the flow path (S-skin; C-core).

To verify the existence of crushed cells and/or cells of small dimension in the skin, an observation was performed in an Ultra-high resolution Field Emission Gun Scanning Electron Microscopy (FEG-SEM), NOVA 200 Nano SEM, FEI Company. The samples were cryo-fractured, sputter coated with gold and fixed in a support with carbon tape adhesive.

2.5 *Gloss*

The gloss measurements were carried with a BYK-Gardner micro-tri-glossmeter calibrated with a black glass standard and according to ASTM D523-85. A minimum of five specimens for each condition and at three different locations in the sample were used to determine the average gloss and respective standard deviation. For each type of surface, the measuring angle was 85º according to the criteria established in this ASTM standard.

2.6 *Roughness*

The topography of the surfaces was assessed with a prototype laser microtopographer (Ferreira et al. 2004). This system does not contact with the surface during measurements, therefore avoiding its damage. It is based on optical active triangulation with oblique incidence and normal (and/or specular) observation, and mechanical scanning of the sample. Five measurements for each condition were carried and each sample was measured in five different locations. The arithmetical average value of roughness, Ra, was determined.

2.7 *Density*

The density was measured using the impulsion method (Archimedes principle) and according with ASTM standard D 792-00. An analytical balance Scaltec SBC 31 (Denver Instrument, Germany) with capacity of 220 g and accuracy of 0.0001 g was used. Together with the balance a density measurement kit was used and the liquid of reference was isopropanol. Five measurements were performed for each condition and an average density value was calculated.

2.8 *Flexural testing*

The flexural tests were performed at room temperature by the three-point support Pouzada and Stevens test method (Pouzada and Stevens 1984). The testing apparatus was mounted in an Instron 4505 universal testing machine (Instron, USA), in compression mode. The samples were placed on the support base and the load was applied at the centre of sample using a crosshead speed of 5 mm/min. A maximum displacement of 5 mm was imposed, guaranteeing that the sample behaved as a plate in the elastic range. The flexural stiffness data hereafter are the average of five tests.

The flexural behaviour of the circular plates in this test is described by the flexural stiffness, C:

$$C = \frac{3R^2B(v)}{4\pi h^3}S_0 \quad (1)$$

where h is the sample thickness, R is the radius of the 3-point support circumference (93.5 mm), B(v) is a function of the Poisson's ratio, v, which in the range of 0.3 to 0.45 has an average value of 5, for HIPS and S_0 is the slope corrected of the load *vs.* displacement curve.

2.9 *Impact test*

The impact tests were performed at room temperature with the CEAST 9350 Fractovis Plus instrumented falling-weight equipment (CEAST, Italy) using the following setup: impact weight of 15.765 kg and drop height of 700 mm, leading to an impact speed of 3.705 m.s^{-1}. The tests were performed according to the European Standard EN ISO 6603-1.

3 RESULTS AND DISCUSSION

3.1 *Mould monitoring*

The mould monitoring data of hybrid and steel mould is depicted as an example in Fig. 3 and 4, respectively. The temperature in the two sides of the mould is different when hybrid mould is used whereas in the steel mould the temperature is very similar. In both cases the injection side of the moulding is always hotter, due to the proximity of the injection nozzle. It is observed an increase of temperature after the injection of the material. The temperature starts decaying slowly until the cooling of the sample is completed. Hybrid mould temperatures (T1 and T2) have a significant difference when the cycle starts and during cooling. The reason for that is related with the different thermal conductivi-

ties of the mould materials used in the core and cavity, which make the cooling rate more difficult to control. In the steel mould the temperatures are similar because the materials have the same thermal properties.

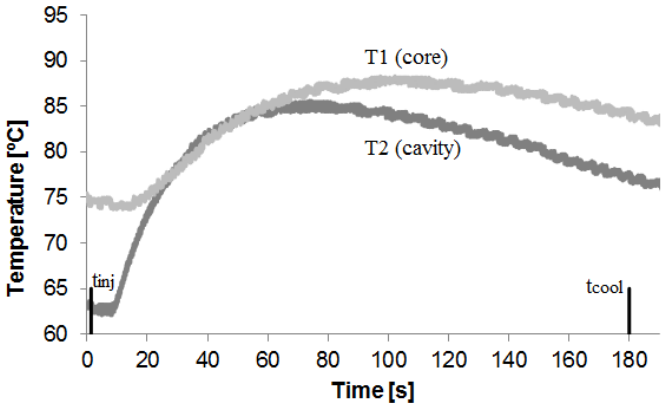

Figure 3. Evolution of temperature in the core (T1) and cavity (T2) sides of the hybrid mould during the injection cycle of HIPS-SF, for T_{inj}= 220ºC.

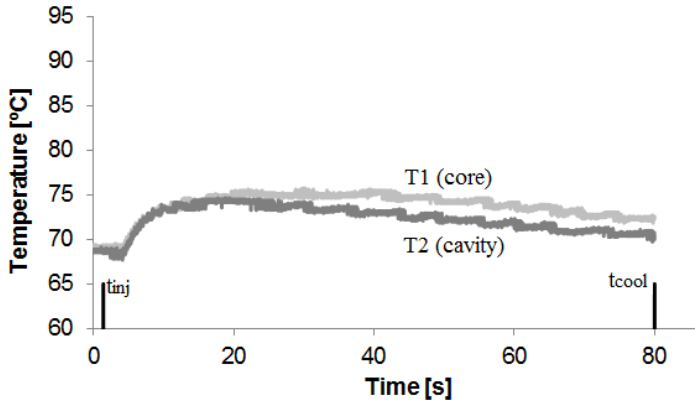

Figure 4. Evolution of temperature in the core (T1) and cavity (T2) sides of the steel mould during the injection cycle of HIPS-SF, for T_{inj}= 220ºC.

3.2 *Morphological characterization*

The typical structure obtained in SF injection moulding is depicted in Fig.5. The structure is characterized by two outer solid layers (skin) and a cellular core. Depending on the type of mould used, different microstructures are developed. With the hybrid mould there is the development of an asymmetric sandwich structure (Fig 5a), b), c)), and in the case of the steel mould the structure is symmetric. This may be related with the variation of the mould temperature during the injection cycle, as shown in the Fig.3 and 4.

The mouldings produced in the hybrid mould also have cells of larger size with a variety of shapes, as compared to the steel one (Fig.5 and 6). In the core, the cells of hybrid mouldings are approximately 200 µm in diameter and the cells of the steel mouldings are only 80 µm. The cells dimensions are decreasing from the centre to the skin due to the difference in the melt temperature and appear distorted as a result of the fountain flow. With the increase of injection temperature, this phenomenon becomes more pronounced. Furthermore, the growth of the cell size is evident with increase of the temperature, due to the lower viscosity and the less resistance to the cell growth (Tovar-Cisneros et al. 2008).

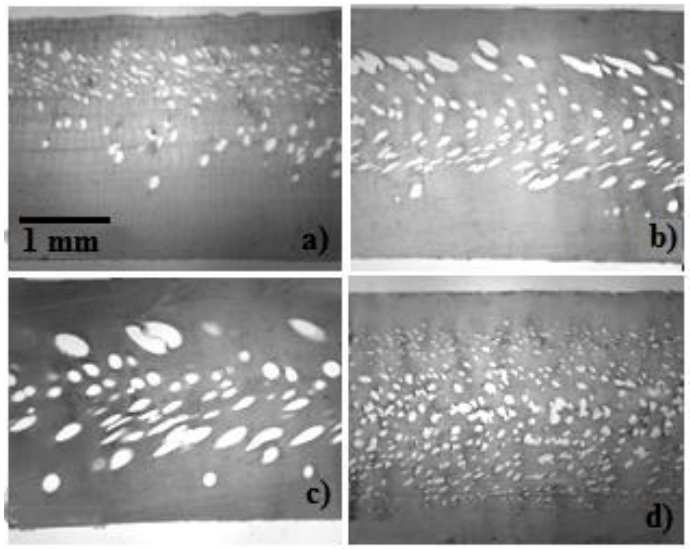

Figure 5. Polarized light microscopy: influence of the injection temperature on the microstructure of HIPS-SF at a) H200; b) H220; c) H240; d) S220.

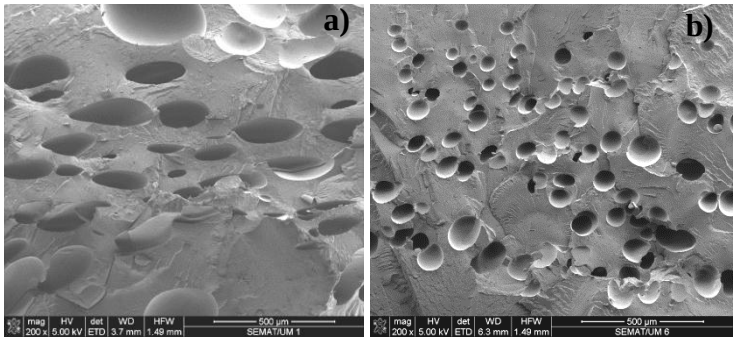

Figure 6. SEM view of the core of the moulding injected in the (a) hybrid mould and (b) steel mould at 220ºC.

In the SEM images it was detected the presence of crushed cells and nanopores in the skin region (Fig.7) which can affect the mechanical properties, mainly the impact behaviour, as it will be shown further.

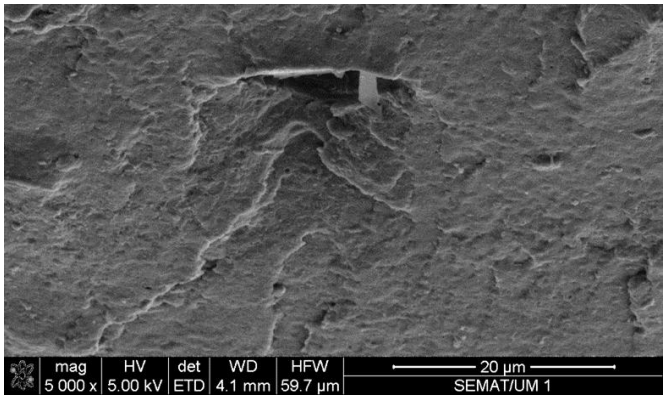

Figure 7. SEM view of the skin of HIPS-SF (H220) with crushed cells and nanopores.

3.3 *Aesthetical analysis*

The surface roughness and, consequently, the gloss of plastics parts are important characteristics that affect the moulding aesthetics. Table 2 and 3 summarise the values of gloss and roughness (R_a), of the moulding blocks and plastics mouldings, respectively. The moulding code is an alphanumeric value, *e.g.*, H200 where the letter means that the material was injected in the hybrid mould (H) or in the steel mould (S), and the number indicates the injection temperature, in this example 200ºC.

Table 2- Roughness and gloss of the moulding blocks.

	Ra [µm]	**Gloss [%]**
Hybrid moulding block	6.96 (1.32)	9.07 (2.24)
Steel moulding block	1.81 (0.40)	59.52 (4.74)

**Standard deviation values are in parentheses.*

Table 3. Effect of the moulding parameters on the gloss and roughness of HIPS-SF.

	HIPS-SF		**HIPS unfoamed**	
	Ra [µm]	Gloss [%]	Ra [µm]	Gloss [%]
H200	1.02 (0.24)	1.69 (0.11)	1.07 (0.19)	1.79 (0.15)
H220	1.10 (0.06)	1.56 (0.16)	2.22 (0.22)	0.98 (0.07)
H240	1.99 (0.38)	0.93 (0.24)	3.70 (0.78)	0.56 (0.17)
S220	0.89 (0.11)	14.74 (2.74)	0.60 (0.17)	47.92 (2.56)

**Standard deviation values are in parentheses.*

The surface finish of the moulding blocks and the processing conditions affected the gloss of the corresponding surface of the moulded parts. The hybrid moulding blocks have R_a higher than the steel blocks. Consequently, the parts produced in the hybrid mould have a higher R_a and consequently a lower gloss due to the replication of the surface roughness of the mould in the plastic part (Oliveira et al. 2006).

The roughness increases with the increase of injection temperature. This may result from the lower viscosity of the material enabling better replication of the rough surfaces (Oliveira et al. 2006; Vasconcelos et al. 2006). HIPS-SF presents lower values of Ra and higher gloss because the pressure required to fill the impression with the expansion of the blowing agent is lower than in conventional mouldings of unfoamed HIPS (Nogueira et al. 2011). So, the replication with HIPS-SF is less accurate than unfoamed HIPS.

3.4 *Flexural behaviour*

Any mechanical property can be related with morphological characteristics such as density profile and skin ratio (Barzegari and Rodrigue 2009a). Table 4 shows the flexural stiffness, skin ratio and density data of HIPS-SF for various processing conditions. The flexural stiffness, skin ratio and density data present average variations of 5%, 9% and 1%, respectively.

Table 4- Flexural stiffness, skin ratio and density of HIPS-SF, for various processing conditions.

HIPS					
	Flexural stiffness [MPa]		Skin ratio [%]	Density [$Mg.m^{-3}$]	
	SF	100%	SF	SF	100%
H200	2277.36 (119.47)	2614.40 (164.92)	44.86 (3.7)	0.94 (0.014)	1.028
H220	2236.76 (88.49)	2568.45 (14.25)	49.36 (5.6)	0.89 (0.005)	1.029
H240	2132.03 (135.77)	2542.27 (51.00)	43.73 (7.5)	0.88 (0.002)	1.027
S220	2081.14 (190.00)	2326.56 (93.82)	29.55 (2.6)	0.86 (0.004)	1.028

In general, increasing the injection temperature decreases the skin ratio and the density. The density is related with the amount and distribution of material available to support the applied loads (Lanz et al. 2002) and therefore as it decreases, the flexural stiffness also decreases. The HIPS-SF mouldings in the hybrid mould are slightly stiffer than in the steel mould, due to the higher skin ratio and density.

3.5 *Impact behaviour*

Fractured HIPS-SF mouldings are shown in Fig. 9.

Figure 9. Fractured HIPS-SF mouldings.

The observation of the crack suggests a ductile fracture, as the crack did not propagate in the radial direction as seen in Fig. 9.

The effect of the injection temperature on the peak energy is shown in Fig. 10.

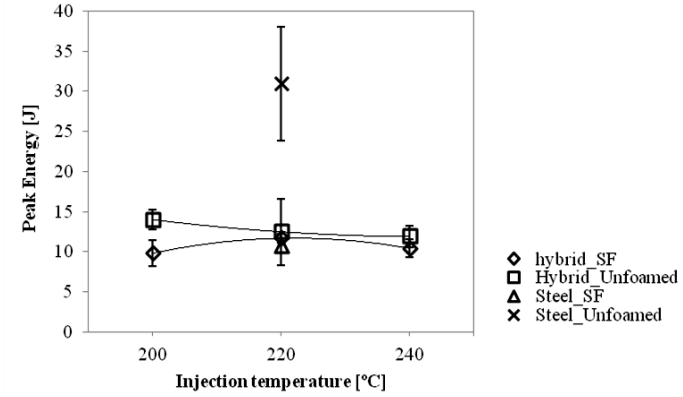

Figure10. Falling weight impact peak energy of HIPS-SF.

As with the flexural properties of HIPS-SF, the falling weight impact resistance is also influenced by the density and the skin thickness. In addition, defects on or near the surface are thought to have major role in determining the peak energy. Raising the injection temperature decreases the peak energy, in accordance to the density reduction.

The occurrence of microcells near to the outer skins may affect the integrity of these outer layers, acting as stress raisers, thus decreasing the impact resistance. The resistance to crack propagation is worst by the formation of large non-uniform cells in the core of the specimens, becoming increasingly evident at high melt temperatures (Ahmadi and Hornsby 1985).

3.6 *Model prediction*

There are analytical models for predicting the mechanical properties once physical and morphological characteristics are known. Barzegari *et al*. proposed a model to predict the flexural behaviour staring with approximations to the density profile (Barzegari M. P. 2007). To simplify notations, they used normalized parameters, as relative density *R*, and relative thickness, *r*:

$$\frac{\rho_c}{\rho_s} = R_1;\ \frac{\rho_f}{\rho_s} = R_2 \qquad (2)$$

$$\frac{\delta_c}{\delta_f} = r\ ;\ \frac{\delta_s}{\delta_f} = 1 - \frac{\delta_c}{\delta_f} = 1 - r \qquad (3)$$

where ρ_f, ρ_s, ρ_c are densities of foam, skin and core, respectively. And δ_f, δ_s, δ_c are thicknesses of foam, skin and core, respectively.

Some of those density variation approaches are shown in Fig. 11. These cross-sections represent an approximation of the density profile along the thickness. In this study, the models of Fig. 11*c* and *d* are analysed.

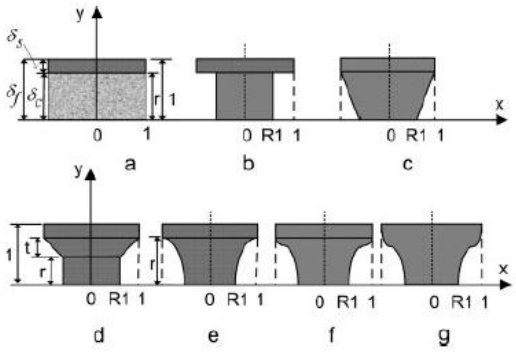

Figure 11. Different approaches of density profiles for SF.

The core density was calculated using the following equations:

$$\left(\frac{\rho_c}{\rho_s}\right) = \left(\frac{\rho_f}{\rho_s} - \frac{\delta_{st}}{\delta_f}\right)\left(1 - \frac{\delta_{st}}{\delta_f}\right)^{-1} \qquad (4)$$

$$\delta_{st} = \delta_{s1} + \delta_{s2}$$

where δ_{st} is the total skin thickness.

Model C. This model assumes that the core density reaches a minimum at the centre of the beam with a linear variation in the core part. Thus, the normalized flexural modulus is obtained by:

$$\frac{E_f}{E_s} = 1 - \frac{r^3}{10}(4 - 3R_1 - R_1)^2 \qquad (5)$$

Model D. The cross-section of Fig. 11d is decomposed into a three-layer structure. It assumes that the skin density decreases linearly to the core density. An intermediate layer, t, is considered and the core density is uniform. Thus, the normalized flexural modulus is:

$$\frac{E_f}{E_s} = 1 - r^3\left(1 - {R_1}^2\right) - r^2 t\left(2 - R_1 - {R_1}^2\right) - rt^2\left(\frac{3}{2} - R_1 - \frac{{R_1}^2}{2}\right) - \frac{t^3}{10}(4 - 3R_1 - {R_1}^2) \qquad (6)$$

Upon using these models, the predicted flexural stiffness can be calculated and the results are presented in Table 5. The predictions using model D are not too far from the experimental, with a maximum error of 9%, whereas with model C, the maximum error is about 14%.

Table5. Prediction of flexural stiffness.

	Experimental	Predictions			
		$C_{Model\ C}$ [MPa]	$C_{Model\ D}$ [MPa]	ΔC_C [%]	ΔC_D [%]
H200	2277	2582	2489	11.78	8.51
H220	2237	2529	2422	11.54	7.64
H240	2132	2490	2350	14.38	9.27
S220	2081	2235	1987	6.88	4.51

CONCLUSIONS

The processing conditions have influence on the aesthetical, morphological and mechanical properties of HIPS-SF mouldings injected in hybrid and steel moulds.

The mouldings in hybrid moulds have reduced gloss due to the higher roughness. The injection temperature has influence on the skin ratio and shape of the cells. With increasing of injection temperature there is an increase of the cell size due to the lower viscosity and a decrease of the skin ratio and density, which makes the flexural stiffness also to decrease.

The mouldings subjected to impact show a ductile behaviour and the peak energy decreases with the increasing temperature.

The mechanical behaviour can be predicted using analytical models based on morphological properties. The predictions are close to the experimental data, with errors less than 10%, for the best model.

ACKNOWLEDGEMENT

The authors acknowledge the support of the program QREN that funded the contract 2010/013307 - project 'Hybridmould 21'.

REFERENCES

Ahmadi, A. A. & Hornsby, P. R. 1984. Moulding and Characterization studies with polypropylene structural foam. I. Structure-property interrelationships. *Plast. Rubber Process. Appl.* **5** (1): 35-49.

Ahmadi, A. A. & Hornsby, P. R. 1985. Moulding and characterization studies with polypropylene structural foam. II. The Influence of Processing Conditions on Structure and Properties. *Plast. Rubber Process. Appl.* **5** (1): 51-59.

Bareta, D. R., Pouzada, A. S. & Costa, C. A. 2007. The effect of rapid tooling materials on mechanical properties of tubular mouldings. In *PMI 2007 - Int. Conf. on Polymers & Moulds Innovations*; Ghent, Belgium, April

Barzegari M. P., D. R. 2007. The effect of density profile on the flexural properties of structural foams. *Polymer Engineering & Science*.

Barzegari, M. R. & Rodrigue, D. 2009a. The Effect of Injection Molding Conditions on the Morphology of Polymer Structural Foams. *Polymer Engineering and Science* **49, 5**: 949-959.

Barzegari, M. R. & Rodrigue, D. 2009b. Flexural behavior of asymmetric structural foams. *Journal of Applied Polymer Science* **113**: 3103-3112.

Ferreira, E. C., Costa, M. F., Laranjeira, C. R., Oliveira, M. J. & Pouzada, A. S. 2004. Comparative study, by optical techniques of the interface polymer/steel in replication conditions. *Advanced Materials Forum II* **455-456**: 467-471.

Kamal, M. R., Isayev, A. I. & Liu, S.-J. 2009. *Injection Molding - Technology and Fundamentals*, Munich: Carl Hanser Verlag.

Lanz, R. W., Melkote, S. N. & Kotnis, M. A. 2002. Machinability of rapid tooling composite board. *Journal of Materials Processing Technology* **127** (2): 242-245.

Malloy, R. A. 1994. *Plastic part design for injection molding: An introduction*, New York: Hanser Publishers.

Mark, J. E. 2007. "Physical properties of polymers handbook." Springer Science + Business Media, New York.

Nogueira, A. A., Martinho, P. G., Brito, A. M. & Pouzada, A. S. 2011. A study on the mouldability of technical parts using hybrid moulds and structural foams. In P. J. Bártolo (ed.), *Innovative Developments in Virtual and Physical Prototyping*: 399-404, London: CRC Press/Balkema.

Oliveira, M. J., Brito, A. M., Costa, M. C. & Costa, M. F. 2006. Gloss and surface topography of ABS: A study on the influence of the injection molding parameters. *Polymer Engineering & Science* **46** (10): 1394-1401.

Pouzada, A. S. 2009. Hybrid moulds: a case of integration of alternative materials and rapid prototyping for tooling. *Virtual and Physical Prototyping* **4** (4): 195 - 202

Pouzada, A. S. & Stevens, M. J. 1984. Methods of generating flexural design data for injection moulded plates. *Plastics and Rubber Processing and Applications* **4** (2): 181-187.

Rosato, D. V., Rosato, D. V. & Rosato, M. G. 2000. *Injection Molding Handbook*, New York: Springer.

Tovar-Cisneros, C., González-Núñez, R. & Rodrigue, D. 2008. Effect of Mold Temperature on Morphology and Mechanical Properties of Injection Molded HDPE Structural Foams. *Journal of Cellular Plastics* **44** (3): 223-237

Vasconcelos, P. V., Jorge Lino, F. & Neto, R. J. 2004. Importance of the Vacuum in Rapid Tooling of Polymeric-Based Moulds. In *RPD-Rapid Product Development*; Marinha Grande, 12 a 13/10/2004.

Vasconcelos, P. V., Jorge Lino, F., Neto, R. J. & Paiva, R. 2006. Design Epoxy Resins Based Composites for Rapid Tooling Applications. In *5th Int. Conf. on Mechanics and Materials in Design*; Porto, Portugal, July 2006.